**Supplemental**

# Atomic-Resolution 1.3 Å Crystal Structure, Inhibition by Sulfate, and Molecular Dynamics of the Bacterial Enzyme DapE

Matthew Kochert[a§], Boguslaw P. Nocek[b], Thahani S. Habeeb Mohammad[a], Elliot Gild[a], Kaitlyn Lovato[a], Tahirah K. Heath[a], Richard C. Holz[c], Kenneth W. Olsen[a]*, and Daniel P. Becker[a]*

*[a]Department of Chemistry and Biochemistry, Loyola University Chicago, 1032 West Sheridan Road, Chicago, IL 60660; [b]The Center for Structural Genomics of Infectious Diseases, Computation Institute, University of Chicago, Chicago, Illinois, 60637; [c]Department of Chemistry, Colorado School of Mines, 1500 Illinois St., Golden, CO 80401, U.S.A.*

Corresponding Authors
Email: kolsen@luc.edu
E-mail: dbecke3@luc.edu

**Table of Contents**

**Table S1**: X-Ray Data Collection and Refinement Statistics

| | |
|---|---|
| <u>Data Collection</u> | |
| Beamline | SBC19-ID (APS) |
| Wavelength (Å) | 0.9795 |
| Resolution range (Å) | 40.00 – 1.30 (1.32 – 1.30) |
| Space group | $P2_12_12_1$ |
| Unit cell | 74.767Å, 88.644Å, 133.402Å<br>90.0°, 90.0°, 90.0° |
| Total no, of reflections | 1603032 |
| No. of unique reflections | 217263 |
| Multiplicity | 7.4 (7.0) |
| Completeness (%) | 99.4 (99.1) |
| Mean I/σI | 21.70 (1.40) |
| Wilson B factor | 13.59 |
| $R_{merge}$, | 0.08000 |
| | |
| <u>Refinement</u> | |
| $R_{work}$, $R_{free}$ | 0.113 (0.200), 0.153 (0.213) |
| RMSD for bonds (Å) | 0.029 |
| RMSD for angles (°) | 2.43 |
| No. of non-hydrogen atoms | |
| Macromolecule | 5894 |
| Ligands | 30 |
| Solvent | 1128 |
| Protein residues | 751 |
| Ramachandran favored/allowed (%) | 98.0/2.0 |
| Ramachandran outliers (%) | 0 |
| Rotamer outliers (%) | 1.90 |
| Clashscore | 5.40 |
| Average B factor ($Å^2$) | 20.28 |
| Molecule/ligands/solvent (Å) | 17.35/26.08/35.44 |

**Table S2.** List of all 11 DapE structures in the PDB, and presence or absence of zinc(II) atoms, sulfate, and distance of sulfates from active site arginine residues

| PDB ID | Bacterial Species | Crystallization Conditions | # of Zn(II) ions in Active Site | # of Sulfates in Active Site | Distance from Sulfates to Active-site Arginine Residues |
|---|---|---|---|---|---|
| 1VGY[1] | *Neisseria Meningitidis* | Not reported | 0 | 0 | N/A |
| 3IC1[2] | *Haemophilus Influenzae* | 1 M $(NH_4)_2SO_4$, 0.2 M NaCl, and 0.1 M NaOAc, pH 4.4 | 2 | 1 in Chain A<br><br><br><br>2 in Chain B | Chain A<br>o 3.1 Å to Arg179<br>o 3.0 Å to Arg258<br>o 5.2 Å to Arg178<br>Chain B Sulfate 1<br>o 2.5 Å to Arg178<br>o 4.5 Å to Arg179<br>Chain B Sulfate 2<br>o 3.0 Å to Arg329<br>o 3.0 Å to Arg258 |
| 3ISZ[2] | *Haemophilus Influenzae* | 1 M $(NH_4)_2SO_4$, 0.2 M NaCl, and 0.1 M NaOAc, pH 4.4 | 1 | 1 in Chain A<br><br><br><br>1 in Chain B | Chain A<br>o 2.7 Å to Arg178<br>o 2.9 Å to Arg179<br>o 6.5 Å to Arg258<br>o 6.5 Å to Arg329<br>Chain B<br>o 2.9 Å to Arg178<br>o 2.8 Å to Arg179<br>o 3.7 Å to Arg258<br>o 4.5 Å to Arg329 |
| 4O23[3] | *Neisseria Meningitidis* | 20% (w/v) PEG 3350, 100 mM HEPES (pH 7.5); 0.1 M succinic acid | 1 in Chain A<br>2 in Chain B | 1 in Chain A<br><br>1 in Chain B | Chain A<br>o 3.25 Å to Arg259<br>Chain B<br>o 2.9 Å to Arg259 |
| 4PPZ[3] | *Neisseria Meningitidis* | 15% (w/v) PEG 3350 and 100 mM succinic acid (pH 7.0), 0.2M $Li_2SO_4$, 0.1M HEPES | 2 in Chain A | 1 in Chain A | Chain A<br>o 2.8 Å to Arg259 |
| 4PQA[3] | *Neisseria Meningitidis* | 0.2 M $NH_4OAc$,0.1 M TRIS (pH 8.5); 25% (w/v) PEG 3350 | 2 in Chain A | 1 in Chain A<br>*Captopril is also bound* | Chain A<br>o 2.9 Å to Arg259 |
| 4ONW[4] | *Vibrio Cholerea* | 20% (v/v) 1,4-butanediol:0.1 M NaOAc, pH 4.5 | 0 | 0 | *Only the Catalytic Domain is crystallized in this structure* |
| 4OP4[4] | *Vibrio Cholerea* | 20% (v/v) 1,4-butanediol: 0.1 M NaOAc, pH 4.5 | 2 in Chain A<br>2 in Chain B | 0 | *Only the Catalytic Domain is crystallized in this structure* |
| 4H2K[4] | *Haemophilus Influenzae* | 0.2 M $NH_4OAc$, 0.1 M bis-TRIS, 25% (w/v) PEG 3350, pH 5.5 | 2 in Chain A<br>2 in Chain B | 0 | *Only the Catalytic Domain is crystallized in this structure* |
| 5UEJ | *Neisseria Meningitidis* | 0.2 M $Li_2SO_4$, 0.1 M Tris:HCl, 1.26 M $(NH_4)_2SO_4$, 0.05 M DMSO, pH 8.5 | 2 in Chain A<br>2 in Chain B | 2 in Chain A<br><br><br><br>2 in Chain B | Chain A: Sulfate 1<br>o 3.5 Å to Arg179<br>Chain A Sulfate 2<br>o 4 Å to Arg259<br>Chain B: Sulfate 1<br>o 3 Å to Arg179 |

| | | | | | |
|---|---|---|---|---|---|
| | | | | | Chain B Sulfate 2<br>o 3 Å o Arg259 |
| 5VO3[5] | *Haemophilus Influenzae* | 0.05 M HEPES (pH 7.3), 10.7% (w/v) PEG MME 2000, 8.6% (w/v) PEG 2000, 0.15M HEPES, 0.06 M sodium potassium tartrate | 2 in Chain A<br>2 in Chain B | 0 | *Products-bound closed conformation structure* |

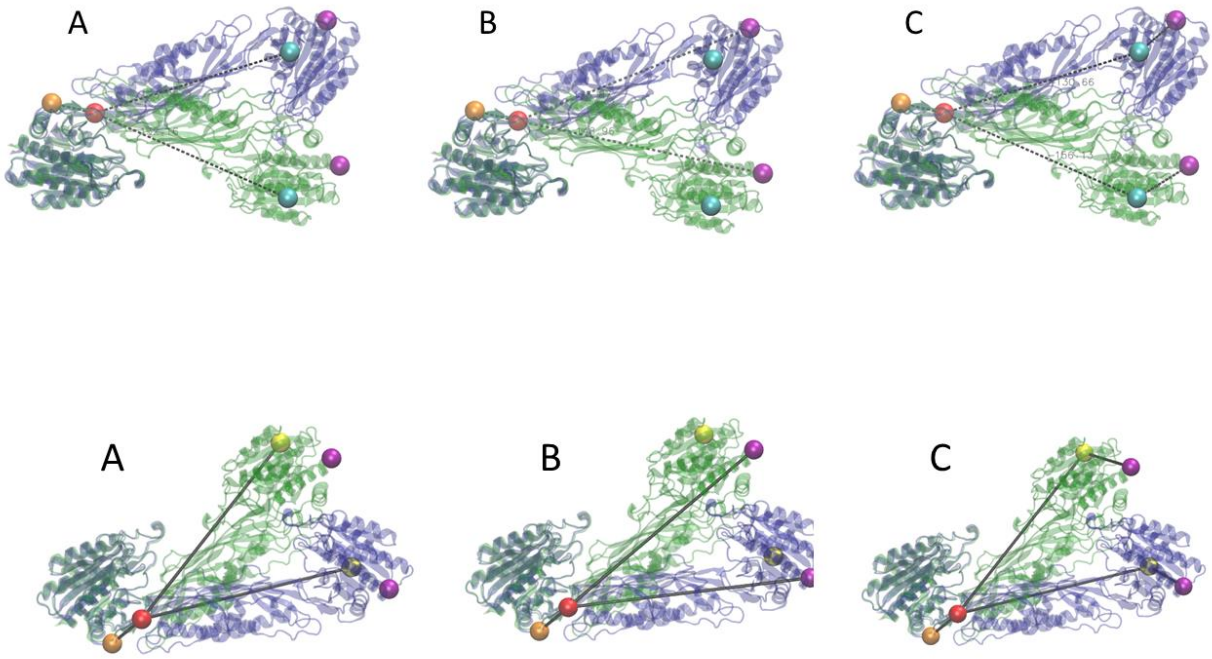


**Figure S1**: Definition of two angles and one dihedral angle to define conformational flexibility of DapE and used in the preparation of Figure S2. A. Angle X is the plane angle formed by the α carbons of residues A299 (designated as an orange sphere in the Figure), A294 (red) and B152 (cyan). This measures the shift in the X direction. B. Angle Y is the plane angle formed by the α carbons of residues A299 (orange), A294 (red) and B376 (purple). This measures the shift in the Y direction. C. Angle Z is the dihedral angle formed by the α carbons of residues A299 (orange), A294 (red), B152 (cyan) and B376 (purple. This measures the shift in the Z direction.

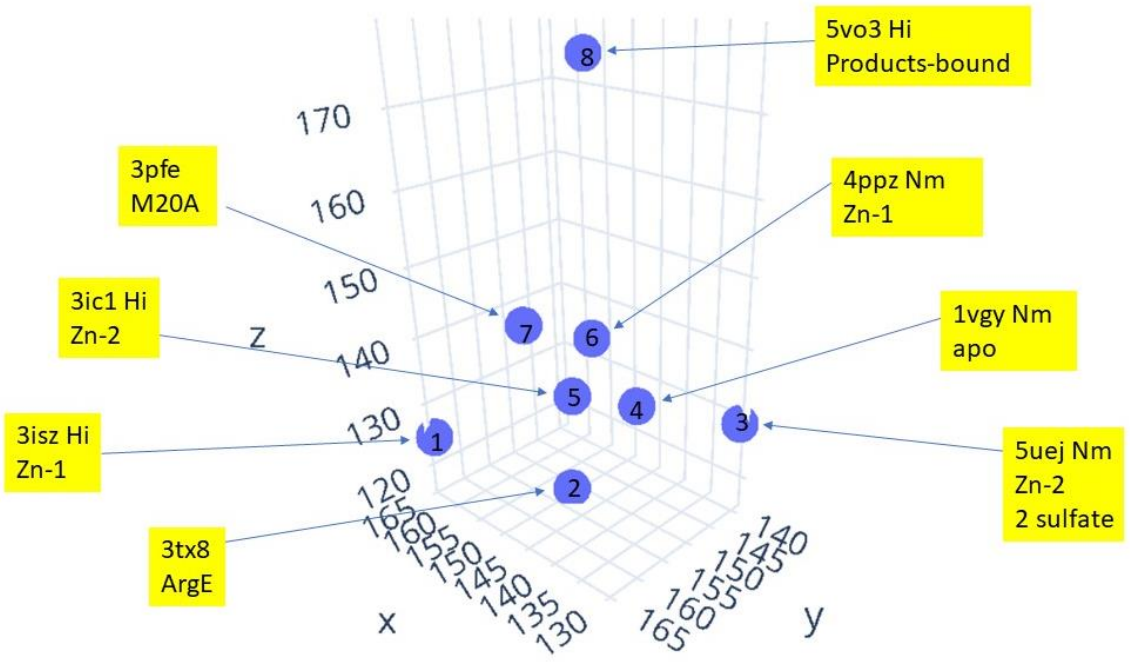


**Figure S2.** 3D plot of angles X, Y and Z plotted for 8 DapE structures, showing the flexibility of the protein when different crystallographic structures are compared. The PDBids are (1) 3ISZ, (2) 3TX8, (3) 5UEJ, (4) 1VGY, (5) 3IC1, (6) 4PPZ, (7) 3PFE and (8) 5VO3. The only closed structure in 5VO3, which is also the only structure to show a significant shift in the Z direction.

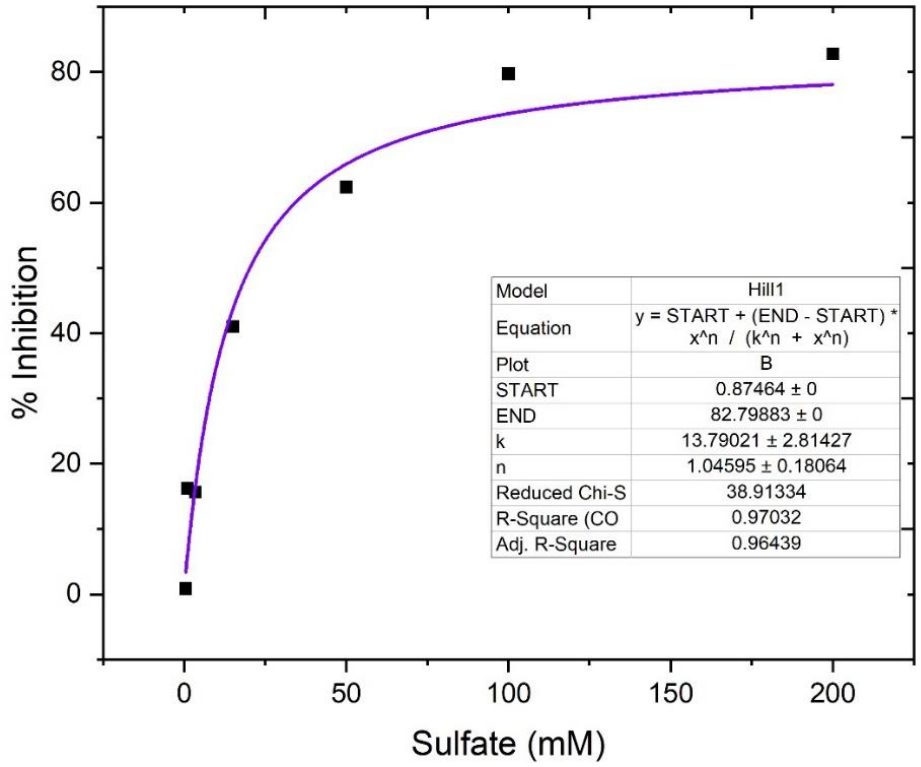


**Figure S3.** $IC_{50}$ curve for lithium sulfate versus DapE. $IC_{50}$ = 13.8 ± 2.81.

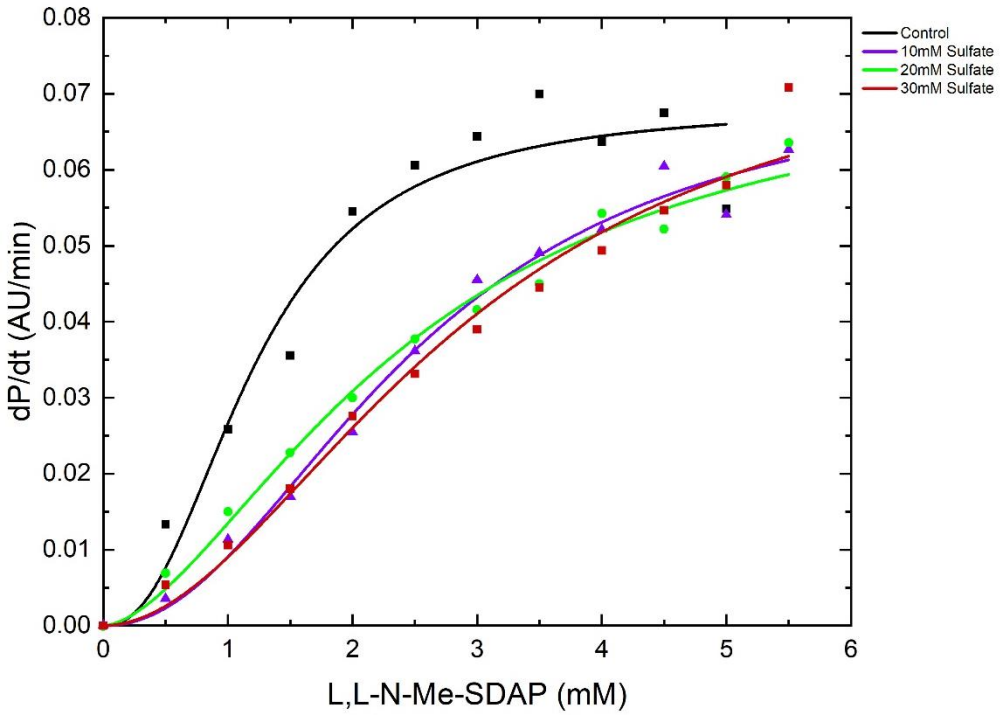


**Figure S4.** *Hi*DapE saturation curves with varying substrate and sulfate concentration.

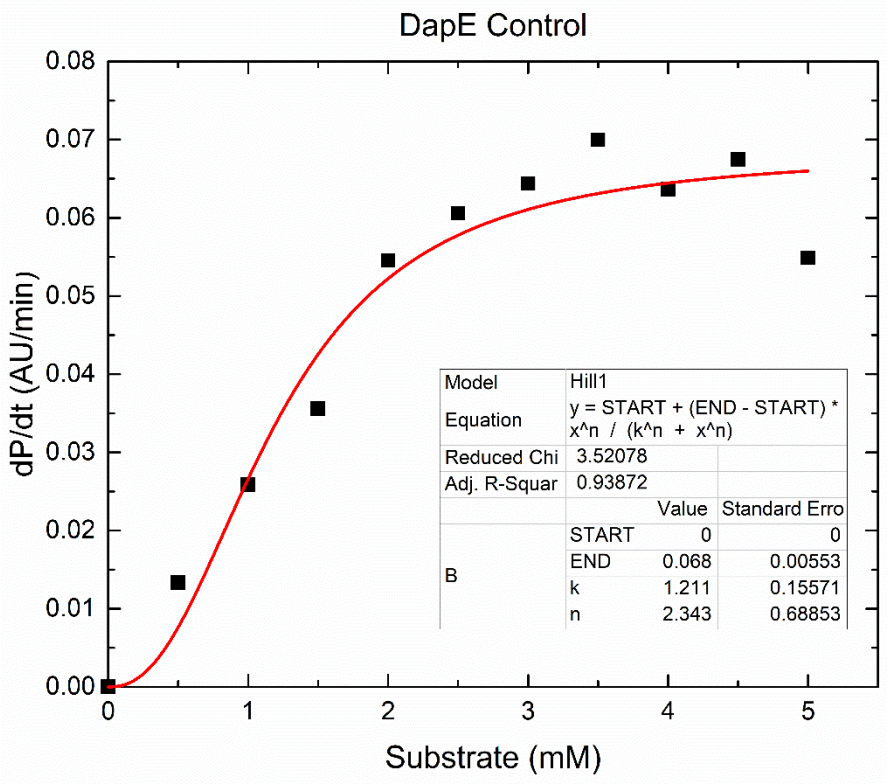


**Figure S5.** *Hi*DapE saturation curve with varying substrate concentration in the absence of sulfate.

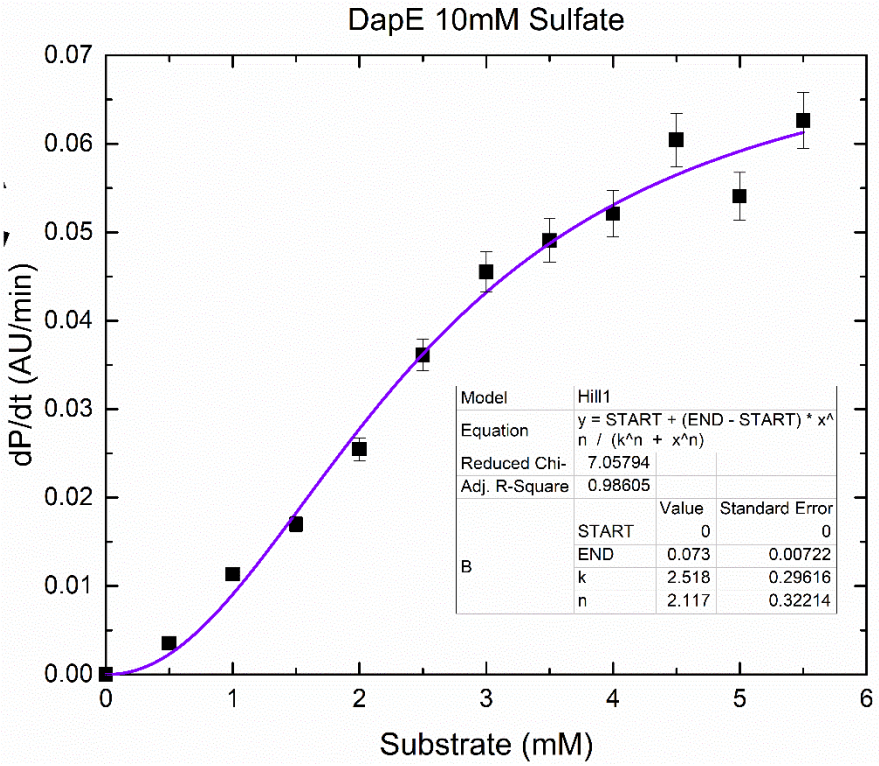


**Figure S6.** *Hi*DapE saturation curve with 10 mM $Li_2SO_4$.

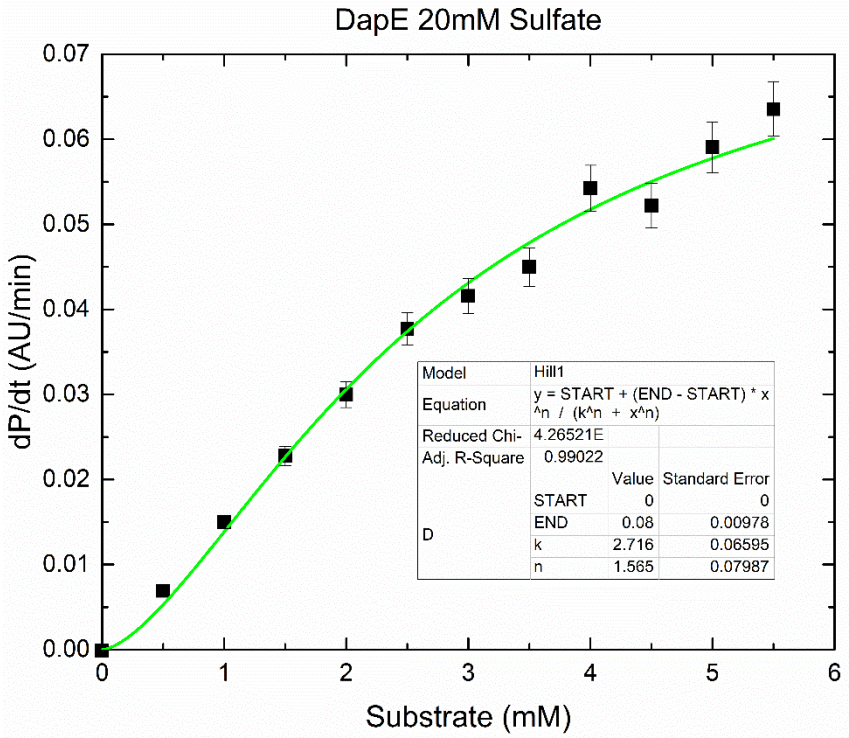


**Figure S7.** *Hi*DapE saturation curve with 20 mM $Li_2SO_4$.

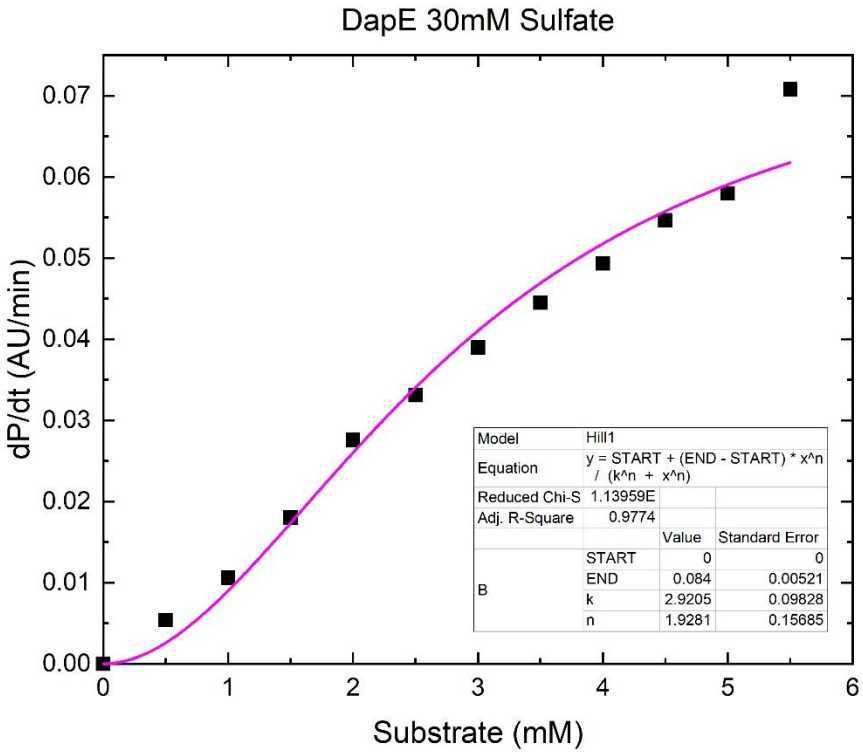


**Figure S8.** *Hi*DapE saturation curve with 30 mM $Li_2SO_4$.

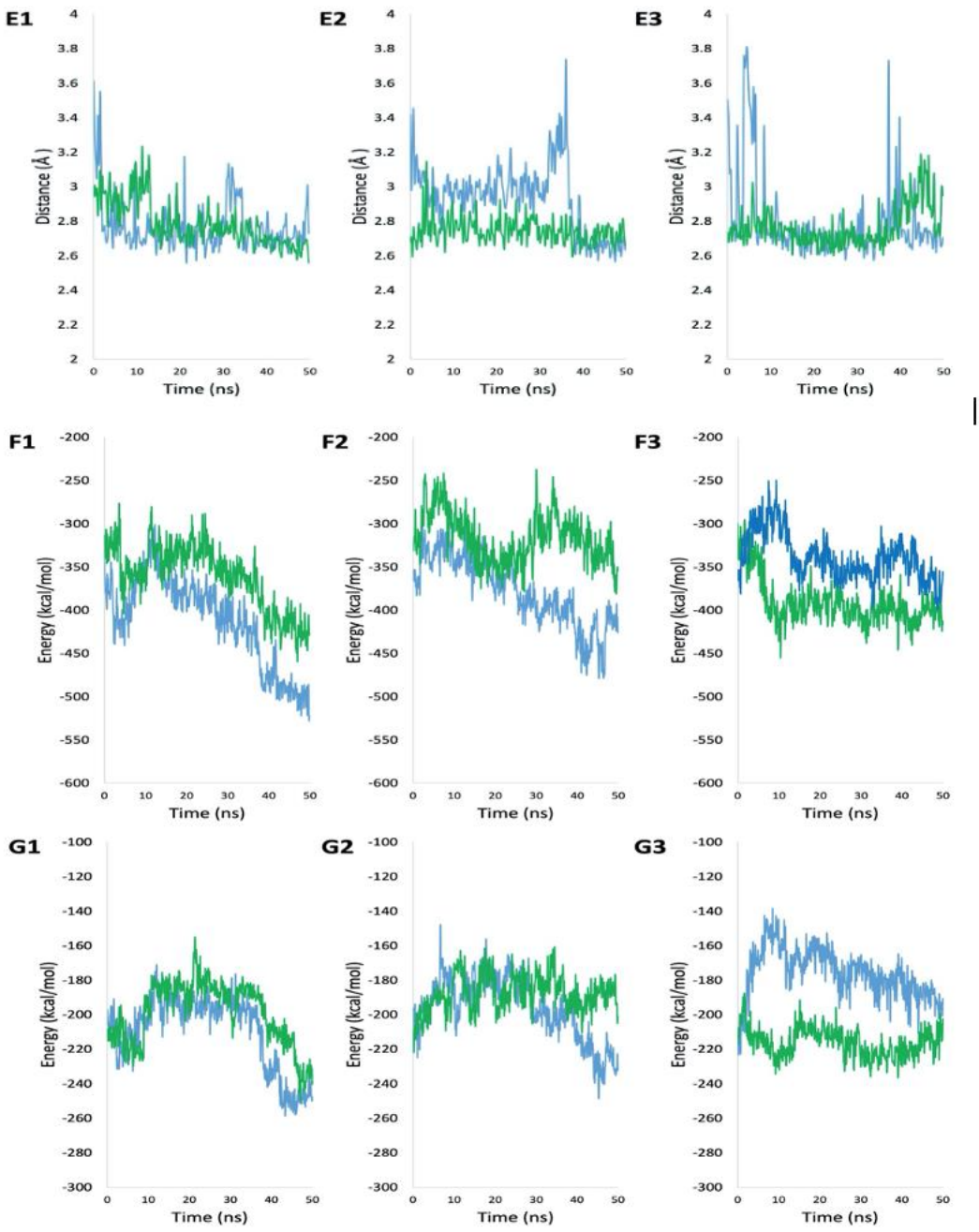


**Figure S9.** (A) Average RMSD from initial to target structure for the simulations with force on (1) both subunits, (2) subunit A, and (3) subunit B. The blue line represents the RMSD for subunit A and the green line represents the RMSD for subunit B. (B) Distances between the amide oxygen in L,L-SDAP and the proximal zinc atom in the active site in the simulations with force on: (1) both subunits, (2) subunit A, and (3) subunit B. The blue lines show the distance in subunit A over time while the green lines show the distance in subunit B over time. (C) Distances between His195 in the communications domain and the proximal zinc atom in the

active site in the simulations with the force on: (1) both subunits, (2) subunit A and (3) subunit B. The blue lines show the distance between His195B and the zinc in subunit A over time while the green lines show the distance between His195A and the zinc in subunit B over time. (D) Distances between Arg179 and L,L-SDAP with the force on: (1) both subunits, (2) subunit A, and (3) subunit B. The blue lines show the distance between Arg179 and the substrate in subunit A over time and the green lines show the distance between Arg179 and the substrate in subunit B over time. (E) Distances between Arg259 and L,L-SDAP with the force on: (1) both subunits, (2) subunit A, and (3) subunit B. The blue lines show the distance between Arg259 and the substrate in subunit A over time while the green lines show the distance between Arg259 and the substrate in subunit B over time. (F) Calculated total interaction energy between the bound substrate and the enzyme in the simulations with force on: (1) both subunits, (2) subunit A and (3) subunit B. The blue lines show the interaction energy between the substrate bound to subunit A and the enzyme and the green lines show the interaction energy between the substrate bound to subunit B and the enzyme. (G) Calculated total interaction energy between the bound substrate and residues Arg179 and Arg259 in the simulations with force on: (1) both subunits, (2) subunit A and (3) subunit B. The blue lines show the interaction energy between the substrate bound to subunit A and the residues and the green lines show the interaction energy between the substrate bound to subunit B and the residues.

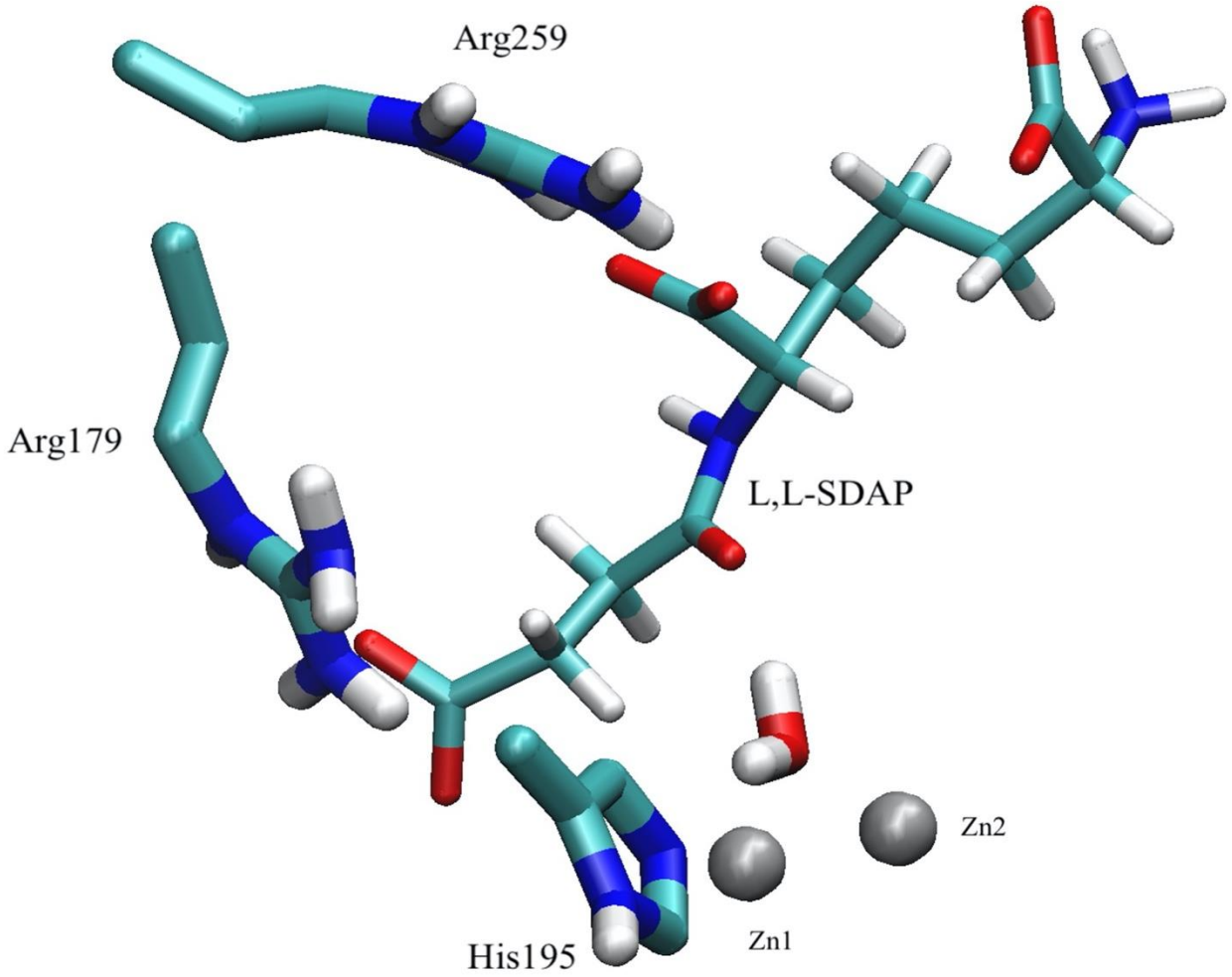


**Figure S10**. Active site of DapE at the end of the TMD simulation in a subunit with force applied. The distance from the active site water molecule to the carbonyl carbon whose amide bond is cleaved by the enzyme is 3.39Å

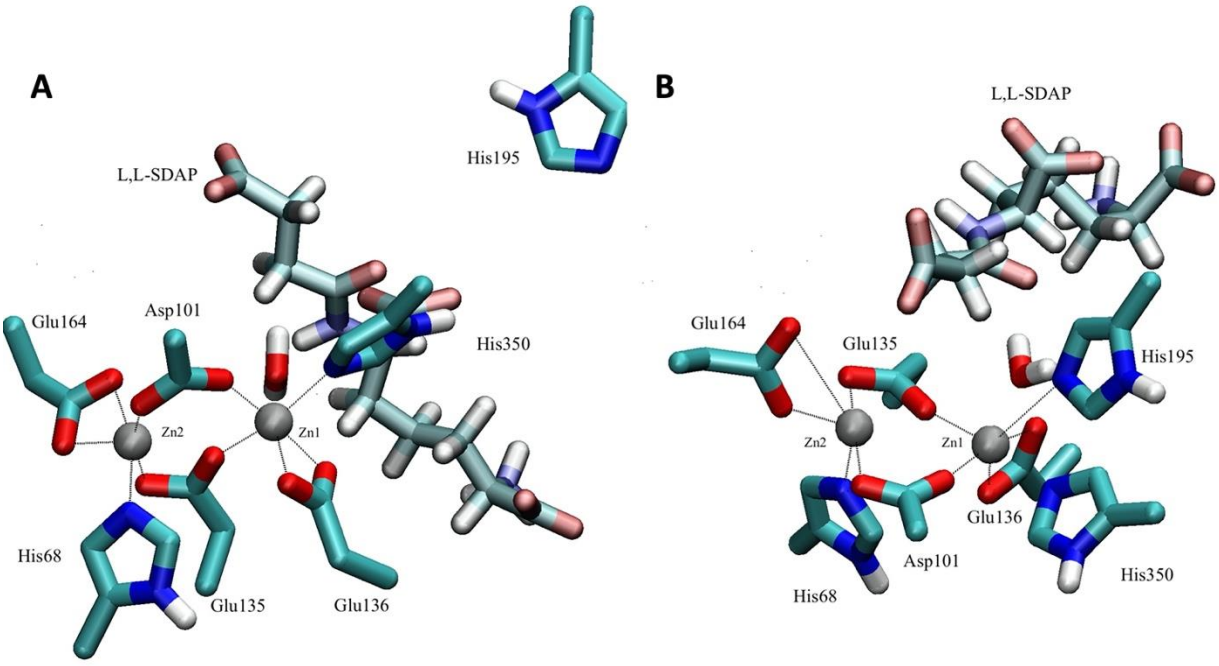


**Figure S11.** Image of the zinc atoms (shown as spheres) in the active site and its coordinated residues at (A) t = 0 and (B) t = 50 ns.

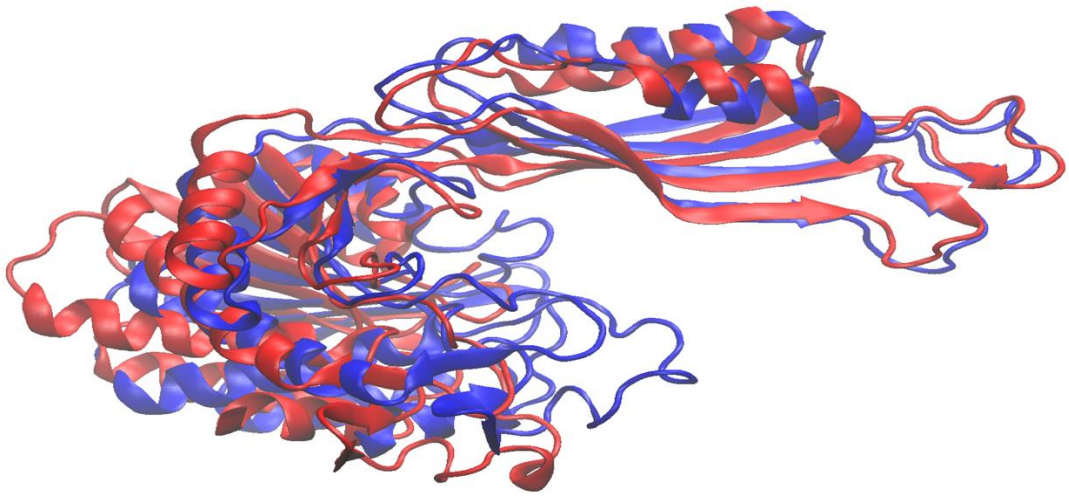

**Figure S12.** Image of a subunit of DapE overlaid at the communications domain at t = 0 (in red) and t = 50 ns (in blue) with the force applied to that subunit.

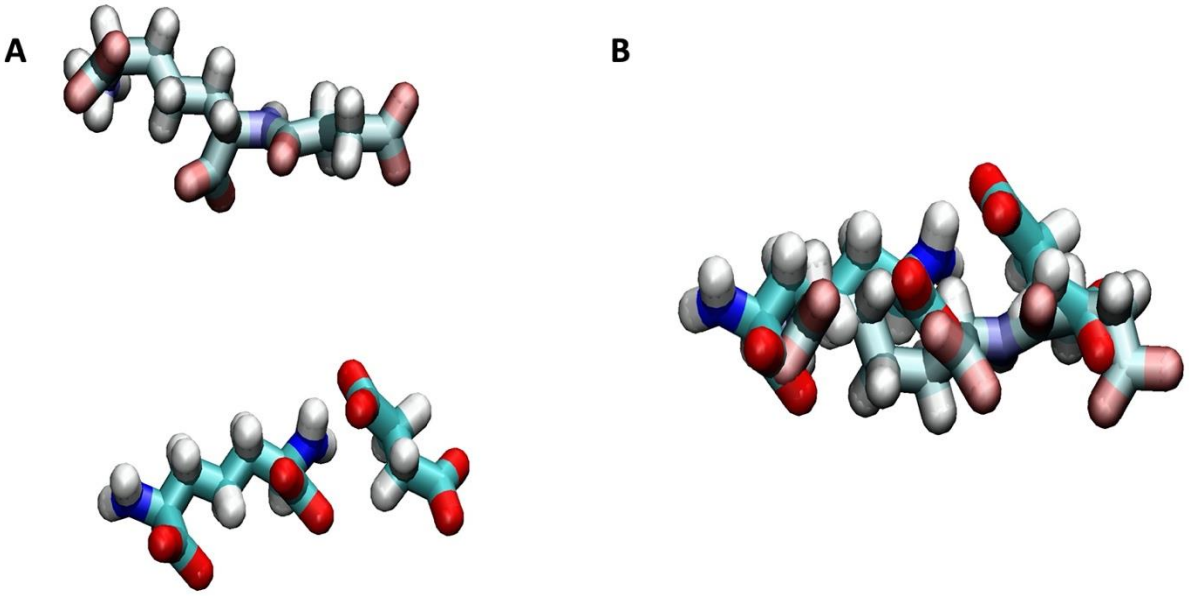


**Figure S13.** Image of the substrate from a subunit with the force applied at (A) t = 0 and (B) t = 50 ns overlaid with the products from the target structure. The substrate moves about 7 Å closer to the position of the products over the simulation as measured from the amide nitrogen in the substrate to the corresponding nitrogen in the product.

**References**

1. Badger, J.; Sauder, J.; Adams, J.; Antonysamy, S.; Bain, K.; Bergseid, M.; Buchanan, S.; Buchanan, M.; Batiyenko, Y.; Christopher, J. Structural analysis of a set of proteins resulting from a bacterial genomics project. *Proteins: Structure, Function, and Bioinformatics* **2005**, *60*, 787-796.

2. Nocek, B. P.; Gillner, D. M.; Fan, Y.; Holz, R. C.; Joachimiak, A. Structural Basis for Catalysis by the Mono- and Dimetalated Forms of the dapE-Encoded N-succinyl-L,L-Diaminopimelic Acid Desuccinylase. *J. Mol. Biol.* **2010**, *397*, 617-626.

3. Starus, A.; Nocek, B.; Bennett, B.; Larrabee, J. A.; Shaw, D. L.; Sae-Lee, W.; Russo, M. T.; Gillner, D. M.; Makowska-Grzyska, M.; Joachimiak, A.; Holz, R. C. Inhibition of the dapE-Encoded N-Succinyl-L,L-diaminopimelic Acid Desuccinylase from Neisseria meningitidis by L-Captopril. *Biochemistry* **2015**, *54*, 4834-4844.

4. Nocek, B.; Starus, A.; Makowska-Grzyska, M.; Gutierrez, B.; Sanchez, S.; Jedrzejczak, R.; Mack, J. C.; Olsen, K. W.; Joachimiak, A.; Holz, R. C. The dimerization domain in DapE enzymes is required for catalysis. *PLoS One* **2014**, *9*, e93593/1-e93593/11, 11.

5. Nocek, B.; Reidl, C.; Starus, A.; Heath, T.; Bienvenue, D.; Osipiuk, J.; Jedrzejczak, R. P.; Joachimiak, A.; Becker, D. P.; Holz, R. C. Structural Evidence for a Major Conformational Change Triggered by Substrate Binding in DapE Enzymes: Impact on the Catalytic Mechanism. *Biochemistry (N. Y. )* **2018**, *57*, 574.